JOURNAL OF AGRICULTURAL AND FOOD CHEMISTRY
ARTICLE

J. Agric. Food Chem. 2009, 57, 9147–9153 9147
DOI:10.1021/jf902507k

Mulberry Leaf Extract Inhibits Vascular Smooth Muscle Cell Migration Involving a Block of Small GTPase and Akt/NF-κB Signals

Kuei-Chuan Chan,[†,§] Hsieh-Hsun Ho,[‡,§] Chien-Ning Huang,[†] Ming-Cheng Lin,[†] Hsiang-Mei Chen,[‡] and Chau-Jong Wang*[,‡]

[†]Department of Internal Medicine, Chung-Shan Medical University Hospital, School of Medicine, Chung-Shan Medical University, No. 110, Sec. 1, Jianguo N. Road, Taichung 402, Taiwan, and [‡]Institute of Biochemistry and Biotechnology, Chung Shan Medical University, No. 110, Sec. 1, Jianguo N. Road, Taichung 402, Taiwan. [§]These authors contributed equally to this work and therefore share first authorship.

Mulberry, the fruit of *Morus alba*, is commonly used in Chinese medicines because of its many pharmacologic effects. Mulberry leaves contain many phenolic antioxidants that can reduce cardiovascular disease. Atherosclerosis involves proliferation and migration of vascular smooth muscle cell (VSMC). Thus, we investigated the mechanisms by which mulberry leaf extract (MLE) might inhibit migration of VSMC. MLE was rich in polyphenols (44.82%), including gallic acid, protocatechuic acid, catechin, gallocatechin gallate, caffeic acid, epicatechin, rutin, and quercetin. MLE could inhibit the migration of A7r5 cells in a dose- and time-dependent manner. MLE also inhibited the activities of matrix metalloproteinases (MMPs) MMP-2 and MMP-9, protein expressions, and phosphorylation of FAK and Akt, and protein expressions of small guanosine triphosphatases (GTPases: c-Raf, Ras, Rac1, Cdc42, and RhoA) in a dose-dependent manner. NF-κB expression was also inhibited by MLE. MLE could effectively inhibit the migration of VSMC by blocking small GTPase and Akt/NF-κB signals.

KEYWORDS: Mulberry leaf extract; atherosclerosis; vascular smooth muscle cell; cell migration

INTRODUCTION

Since 1990, coronary artery disease (CAD) has become the leading cause of death in the United States (*1*). Atherosclerosis is the major cause of CAD, and diets that are rich in phenolic antioxidants reduce cardiovascular disease (*2*). Mulberry leaf, the leaf of *Morus alba*, is commonly used to feed silkworms and has been effectively used in Chinese medicines because of its many pharmacologic effects, including the prevention of CAD (*3*). Dietary mulberry has also been reported to have hypoglycemic (*4*, *5*), hypolipidemic (*6*), and antioxidant (*7*) effects. Mulberry leaf extracts (MLE) have been shown to have inhibitory effects on oxidation of low density lipoprotein (LDL) (*8*) and to prevent atherosclerosis in apolipoprotein E-deficient mice (*9*). Moreover, mulberry leaf therapies for type 2 diabetic patients or streptozotocin-induced diabetic rats have improved fasting blood glucose levels (*10*, *11*).

Understanding the mechanisms underlying vascular smooth muscle cell (VSMC) proliferation and migration is important for evaluating the involvement of these processes in the pathophysiology of atherosclerosis, hypertension, and restenosis. VSMC migration involves many signal transduction proteins. Focal adhesion kinase (FAK) was found to play a role in integrin signaling, which induces many intracellular events, such as rearrangement of the actin cytoskeleton, cell migration, cell survival, and gene expression (*12*). Increasing the expression of FAK will stimulate cell migration (*13*).

The Rho family of small guanosine triphosphatases (GTPases), which include Rho, Rac, and Cdc42, acts as molecular switches to regulate the actin cytoskeleton. Rho and Rho kinase can mediate thrombin-stimulated vascular smooth muscle cell DNA synthesis and migration (*14*). The Rho family of GTPases was also reported to be involved in the regulation of nuclear factor-κB (NF-κB)-dependent transcription.

NF-κB, a family of transcription factors, plays a central role in inflammation, arteriosclerosis, restenosis after percutaneous coronary intervention (PCI), and reperfusion injury, as well angiogenesis (*15*). NF-κB may regulate angiogenesis via the induction of matrix metalloproteinases (MMPs) (*16*). MMP-2 and MMP-9 were found in intimal smooth muscle cells (SMCs) cultured from injured baboon aortas. SMC migration after vessel injury in vivo may be dependent on increased MMP-2 activity, and antisera that neutralized MMP-2 activity inhibited the in vitro migration of SMC by $>80\%$ (*17*).

Phosphoinositide-3-kinase (PI3K) signaling was found to be necessary to mediate the proliferation and migration of human pulmonary vascular smooth muscle cells (*18*). Akt kinase, an important component of postsurvival signaling pathways, is activated via the PI3K signaling pathway (*19*).

*Corresponding author. Tel: 886-4-24730022 ext: 11670. Fax: 886-4- 23248167. E- mail: wcj@csmu.edu.tw.

Published on Web 09/17/2009

Although MLE has been reported to inhibit oxidation of LDL (*8*), an important process during atherosclerosis, and has been previously used to prevent CAD, the effects of MLE on VSMCs migration are still not fully understood. Thus, we investigated the effects and mechanisms by which MLE inhibited the migration of VSMCs.

MATERIALS AND METHODS

Cell Culture. Cell line A7r5, a rat thoracic aorta smooth muscle cell line, was obtained from the ATCC (ATCC number: CRL-1444; Manassas, VA). A7r5 cells were cultured in Dulbecco's modified Eagle's medium (DMEM) supplemented with 10% fetal bovine serum (FBS), 1% glutamine, 1% penicillin−streptomycin, and 1.5 g/L sodium bicarbonate (all from Gibco/BRL; Gaithersburg, MD). All cell cultures were maintained at 37 °C in a humidified atmosphere of 5% CO_2. Before treatment, the cells were precultured in 0.5% FBS medium for 48 h.

Cell Viability Analysis. Cell viability was determined using 3-(4,5-dimethylthiazol-2-yl)-2,5-diphenyltetrazolium bromide (MTT) assays. Cells were seeded in 12-well culture plates at a density of 2×10^5 cells/well and incubated in 0.5% FBS medium for 48 h. Then, MLE at varying concentrations (0.5, 1.0, 1.5, and 2.0 mg/mL) was added for 24 h to evaluate any dose-dependent effects of MLE on VSMC growth and viability. After this, 0.5 mg/mL MTT was added, and cells were cultured at 37 °C in a humidified atmosphere of 5% CO_2 for another 4 h. Following solubilization with isopropanol, the viable cell number was directly proportional to the production of formazan measured spectrophotometrically at 563 nm.

Growth Curves. A7r5 cells were seeded into 6-well culture plates at a density of 5×10^5 cells/well. When cells had grown up to 80% confluence, the cells were precultured in 0.5% FBS medium for 48 h. Then, MLE at doses of 0.0, 0.5, 1.0, 1.5, and 2.0 mg/mL were added to the culture medium. The cell numbers were counted using a cellular counting plate each day for 7 days. On the basis of the mean values of the cells in these wells, growth curves were generated. Results are representative of at least 3 independent experiments.

Extraction of Aqueous Fractions from Mulberry Leaves. Fresh mulberry leaves (100 g) were harvested and immediately dried at 50 °C. The dried leaves were heated in 1500 mL of deionized water. After filtration, we removed the residue. The suspension was stored at −80 °C overnight. Then, we used a freeze-dryer (Labconco) to evaporate the suspension to powder. The dried powder was the aqueous fraction of MLE.

HPLC (High Performance Liquid Chromatography) Assay. The components of MLE were determined by HPLC analysis using a Hewlett-Packard Vectra 436/33N system with a diode array detector. The HPLC method employed a 5 μm RP-18 column (4.6 × 150 mm i.d.). The MLE was filtered through a 0.22 μm filter disk, and then 25 mg/mL of MLE was injected into the column. Chromatography was monitored at 280 nm, and UV spectra were collected to confirm peak purity. The mobile phase contained two solvents: A, 2% acetic acid/water; B, 0.5% acetic acid in water/acetonitrile.

Total Phenolic Content Assay. Total phenolic compound content in each extract was spectrophotometrically determined in accordance with the Folin−Ciocalteu procedure by reading the absorbance at 725 nm against a methanol blank. Briefly, samples (20 μL, water added to 1.6 mL) were introduced into test tubes, and then 100 μL of Folin−Ciocalteu reagent and 300 μL of sodium carbonate (20%) were added. The tubes' contents were mixed and incubated at 40 °C for 40 min. Absorption at 725 nm was measured. The total phenolic contents were expressed as milligrams per gram of MLE for gallic acid (GA), quercetin, rutin, caffeic acid (CA), and gallocatechin gallate (GCG).

Total Polysaccharide Content Assay (Phenol−Sulfuric Acid Assay). We used the phenol−sulfuric acid method to measure the polysaccharide content. The MLE was diluted in deionized water, and the dissolved extracts were filtered through a 0.22 μm filter (MILLEX-HA) before treatment. Briefly, 100 μL of MLE, 100 μL of phenol (5%), and 500 μL of H_2SO_4 (95.5%) were mixed and then incubated at room temperature for 15 min. The absorbance at 490 nm was used to determine the amount of carbohydrate in the sample. Different concentrations of glucose (0, 10, 30, 50, 70, and 90 μg/mL) were used as standards.

Protein Content Assay. Protein content was measured by the Bradford protein assay. The MLE was diluted in deionized water, and the dissolved extracts were filtered through a 0.22 μm filter (MILLEX-HA) before treatment. Briefly, 100 μL of MLE and 700 μL of Coomassie Brilliant blue were mixed, and then incubated in the dark for 15 min. Then, the absorbance was measured at 595 nm. Different concentrations of BSA (bovine serum albumin) (0, 200, 400, 800, 1200, and 1600 μg/mL) were used as standards.

Lipid Content Assay. Lipid content was measured by the acid hydrolysis method (rapid method). The MLEs (1 g) were mixed with hydrochloric acid (20 mL) in a conical flask, then heated in a water bath at 70−80 °C for about 50 min. After heating, the mixture was cooled to room temperature, and then 10 mL of ethanol and 20 mL of ethyl ether were added to a separatory funnel. The separatory funnel was vigorously shaken to ensure the complete mixing of the two liquid phases. Then, the two liquid phases were allowed to separate for at least 2 h until the layers were clearly separated. The lower solvent was collected in a new beaker, and the upper solvent (ethyl ether) was collected in a conical flask. Ethyl ether (20 mL) was added to the lower solvent and poured into a separatory funnel, which was shaken vigorously to ensure the complete mixing of the two liquid phases. The above process was repeated 3 times. The collected ethyl ether was evaporated under vacuum and then dried in an oven. The weight of the flask was measured and used as the content of lipid after the flask tare weight was subtracted.

Western Blot Analysis. For Western blot analysis, we used specific antibodies to evaluate the expressions of p-FAK, PI3-K (BD, San Jose, CA, USA), c-Raf (Transduction Laboratories, Lexington, KY, USA), Ras, Rac 1, Cdc 42, Rho A, p-Akt, Akt (Santa Cruz, Santa Cruz, CA, USA), and β-actin (Sigma, St. Louis, Mo, USA). After the indicated MLE treatment, equal amounts of cell lysates (50 μg protein) were separated by electrophoresis on 8−12% sodium dodecyl sulfide−polyacrylamide gel electrophoresis (SDS−PAGE) and transferred to nitrocellulose membranes (Millipore, Bedford, Mass, USA). The membranes were incubated with Tris-buffered saline (TBS) containing 1% (W/V) nonfat-milk and 0.1% (V/V) Tween-20 (TBST) for 1 h to block nonspecific binding and then washed with TBST for 30 min. Each membrane was incubated with the appropriate primary antibody for 2 h followed by horseradish peroxidase-conjugated second antibody (Sigma, St. Louis, Mo, USA) for 1 h and developed by ECL chemiluminescence (Millipore, Bedford, Mass, USA), then analyzed using AlphaImager Series 2200 software. Results are representative of at least 3 independent experiments.

Wound Healing Assay. A7r5 cells were seeded in 6-well culture plates and then starved with 0.5% FBS DMEM medium for 48 h. A sterile 100 μL pipet tip was used to make a straight scratch in the cells in each well. The scratched cells were washed out with PBS (phosphate buffered saline), and the remaining cells were treated with MLE at varying concentrations (0.05, 0.1, 0.2, 0.5, and 1.0 mg/mL) at 37 °C in a humidified atmosphere of 5% CO_2. Under a 40× lens, images were taken of 9 fields per well of the linear wound at the following times: 0, 24, 36, 48, 60, and 72 h. Migrated cells were counted per well and averaged.

Boyden Chamber Migration Assay. A7r5 cells were seeded in 6-well culture plates (5×10^5/well), starved with 0.5% FBS DMEM medium for 48 h, and then treated with MLE at varying concentrations (0.1, 0.2, 0.5, 1.0, 1.5, and 2.0 mg/mL) at 37 °C in a humidified atmosphere of 5% CO_2 for 48 h. Then, the cells were detached by trypsinization. Treated cells were seeded into the upper chamber of a Boyden chamber at a density of 1×10^6/chamber in 10% FBS medium and then incubated for 6 h at 37 °C in a humidified atmosphere of 5% CO_2 . Cells that had invaded to the lower surface of the membranes were fixed with methanol for 10 min and stained with Giemsa for 1 h. The cells on the lower side of the membrane were counted and averaged in 4 high-power fields (400×) with a light microscope.

MMP Gelatin Zymography. A7r5 cells were plated onto 6-well culture plates (5×10^5/well) and then starved with 0.5% FBS culture medium for 48 h. The cells were treated with MLE at varying concentrations (0.05, 0.1, 0.2, 0.5, and 1.0 mg/mL) at 37 °C in a humidified atmosphere of 5% CO_2 for 48 h. Additional groups of cells were treated with MLE at a concentration of 0.5 mg/mL for different times (0, 12, 24, 36, or 48 h) at 37 °C in a humidified atmosphere of 5% CO_2. After this, the medium was removed and washed twice with PBS, and 1 mL of 0.1% FBS DMEM was added for 24 h. After treatment, the culture medium was

collected and centrifuged at 12,000 rpm for 5 min at 4 °C to remove cell debris. The prepared samples were subjected to electrophoresis with 8% SDS−PAGE containing 0.1% gelatin. Following electrophoresis, gels were washed twice with 2.5% Triton X-100 on a gyrating shaker for 30 min at room temperature to remove SDS. The gel was then incubated in 50 mL of reaction buffer (40 mM Tris-HCl, 10 mM $CaCl_2$, and 0.01% NaN_3) at 37 °C overnight on a rotary shaker, stained with Coomassie Brilliant blue R-250, then destained with methanol−acetic acid−water (50:75:875, v/v/v). Gelatinolytic activities were detected as horizontal white bands on a blue background.

Electrophoretic Mobility Shift Assay (EMSA). To prepare nuclear extracts, cells were washed with ice-cold PBS and then detached by trypsinization. Reagent A (10 mmol/L HEPES, 10 mmol/L KCl. 0.1 mmol/L EDTA, 1.5 mmol/L $MgCl_2$, 1% NP40, 1 mmol/L DTT, and 0.5 mmol/L phenyl-methylsulfonyl fluoride) was added, and then cell membranes were destroyed by vortexing. After centrifugation at 3000 rpm for 10 min at 4 °C, the suspension was removed, and the pellet was harvested. After this, reagent C (20 mmol/L HEPES, 25% glycerol, 1.5 mmol/L $MgCl_2$, 0.1 mmol/L EDTA, 420 mmol/L NaCl, 1 mmol/L DTT, and 0.5 mmol/L phenyl-methylsulfonyl fluoride) and RIPA buffer (150 mM NaCl, 0.5% deoxycholic acidl, and 50 mM Tris base) were added and then vortexed at 4 °C for 1 h. After centrifugation at 12000 rpm for 10 min at 4 °C, the nuclear extract was obtained. The supernatant was stored at −20 °C .

We prepared a native polyacrylamide gel in 0.5× TBE. TBE−PAGE (4 mL of polyacrylamide 29:1, 1.5 mL of 10× TBE buffer, 3 mL of 50% glycerol, 21.5 mL of ddH_2O, 150 μL 10% ammonium persulfate, and 15 μL TEMED). Then, we flushed the wells and pre-electrophoresed the gel for 60 min at 100 V. We mixed the buffer and DNA probe (2 μL 10× binding buffer, 2 μL 50% glycerol, 1 μL 100 mM $MgCl_2$, 1 μL poly dI/dC, 1 μL biotin-DNA probe, 1 μL 1% NP-40, and 10 μg of nuclear extract), and then deionized water was added up to 20 μL. A binding reaction was performed at room temperature for 15 min, and then 5 μL of loading buffer was added. After electrophoresis, the TBE−PAGE was transferred to a nylon membrane, which was cross-linked by UV-light (1200 mJ for 2 times). To block the membrane, we added 20 mL of blocking buffer (LightShift Chemiluminescent EMSA Kit, Pierce, Rockford, IL, U.S.A.) and incubated for 15 min with gentle shaking. Then, we added HRP (horseradish peroxidase) conjugate in blocking buffer (1:600 dilution) (Pierce) with gentle shaking for 20 min. The nylon membrane was washed 3 times with 1× wash buffer (Pierce) for 10 min for each wash. After this, we added substrate buffer (Pierce) and incubated for 15 min, then developed by using ECL chemiluminescence (Millipore, Bedford, Mass, USA). AlphaImager Series 2200 software was used. Results are representative of at least 3 independent experiments.

Statistical Analysis. Results are reported as the means ± standard deviation of 3 independent experiments, and statistical comparisons were evaluated by one-way analysis of variance (ANOVA). $P < 0.05$ was considered statistically significant.

Table 1. Composition of MLE[a]

MLE	%
polyphenol	23.60
polyphenol	44.82
polysaccharide	27.73
protein	2.33
lipid	8.40

[a] MLE: mulberry leaf extract. [b] Gallic acid as the standard of polyphenol content assay. [c] Quercetin as the standard of polyphenol content assay.

Table 2. Composition of Polyphenol and Phenoic Acid Separated from MLE[a]

component	RT (min)	MLE (%)
gallic acid	7.98	7.64
protocatechuic acid (PCA)	15.36	4.69
catechin	21.71	1.20
gallocatechin gallate (GCG)	24.78	5.88
caffeic acid	27.42	1.02
epicatechin	29.32	0.80
rutin	38.43	1.87
quercetin	56.86	1.24
naringenin	60.54	2.67

[a] The MLE was prepared as described in Materials and Methods. MLE: mulberry leaf extract.

RESULTS AND DISCUSSION

Components of MLE. The yield of MLE was 38.63%. **Table 1** shows the major components of MLE, including polyphenols (23.60%, gallic acid as the standard), polyphenols (44.82%, quercetin as the standard), polysaccharide (27.73%), protein (2.33%), and lipid (8.4%). **Table 2** shows the composition of polyphenol and phenoic acids separated from MLE, including gallic acid (7.64%), protocatechuic acid (4.69%), catechin (1.2%), gallocatechin gallate (5.88%), caffeic acid (1.02%), epicatechin (0.8%), rutin (1.87%), quercetin (1.24%), and naringenin (2.67%). **Figure 1** shows the HPLC chromatogram of MLE. This included 9 types of standard polyphenols and phenolic acids (0.5 mg/mL). The effect of MLE on A7r5 cells viability was determined by the MTT assay. As shown in **Figure 2**,

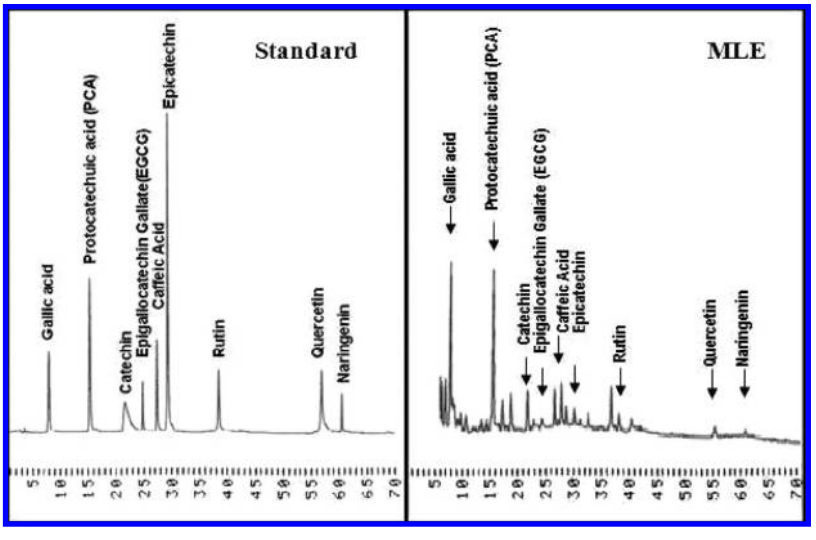

Figure 1. HPLC chromatogram of MLE. HPLC chromatograms of MLE (25 mg/mL) showed that there were nine kinds of standard polyphenols and phenolic acids (0.5 mg/mL) within it. The arrow indicates the retention time (RT) of polyphenols or phenolic acids.

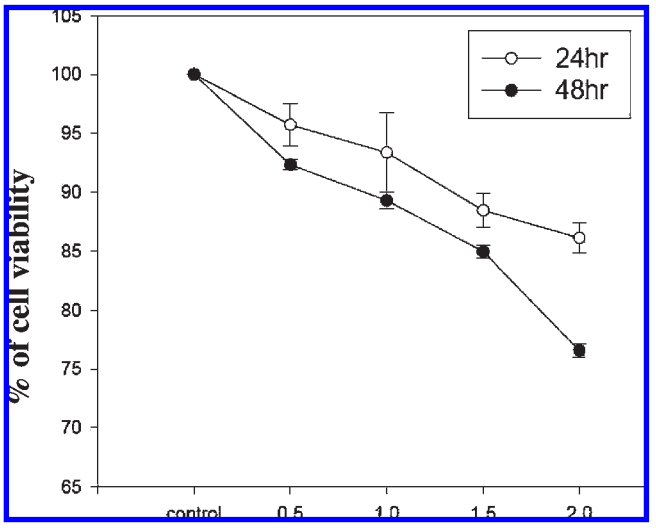

Figure 2. MTT assay of the effect of MLE on rat aortic smooth muscle cell (A7r5) viability. MLE had a significant inhibitory effect on VSMC growth in a dose- and time-dependent manner. The data were the means ± SD from 3 samples for each group.

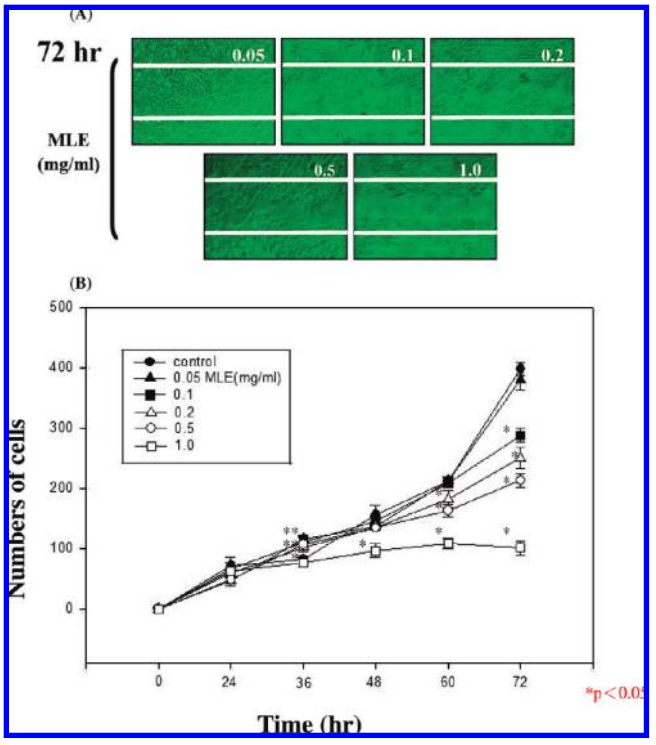

Figure 3. Effect of MLE on the migration of A7r5 cells by the wound healing assay. (**A**) Cell number in the denuded zone (i.e., wound) decreased as concentrations of MLE increased. White lines indicate the wound edge. (**B**) MLE inhibited cell migration in a dose-dependent manner. Data are reported as the means ± SD of 3 independent experiments. (*$p < 0.05$, as compared with that of the control group).

MLE had a significant inhibitory effect on VSMC growth in a dose-dependent manner following 24 and 48 h of incubation with 0.5−2.0 mg/mL of MLE.

Noncytotoxic Doses of MLE Inhibited VSMC Migration. Previous studies have indicated that proliferation and migration of smooth muscle cells contributed to the development of atherosclerosis. To evaluate the effects of MLE on smooth muscle cell migration, wound healing and Boyden chamber migration assays

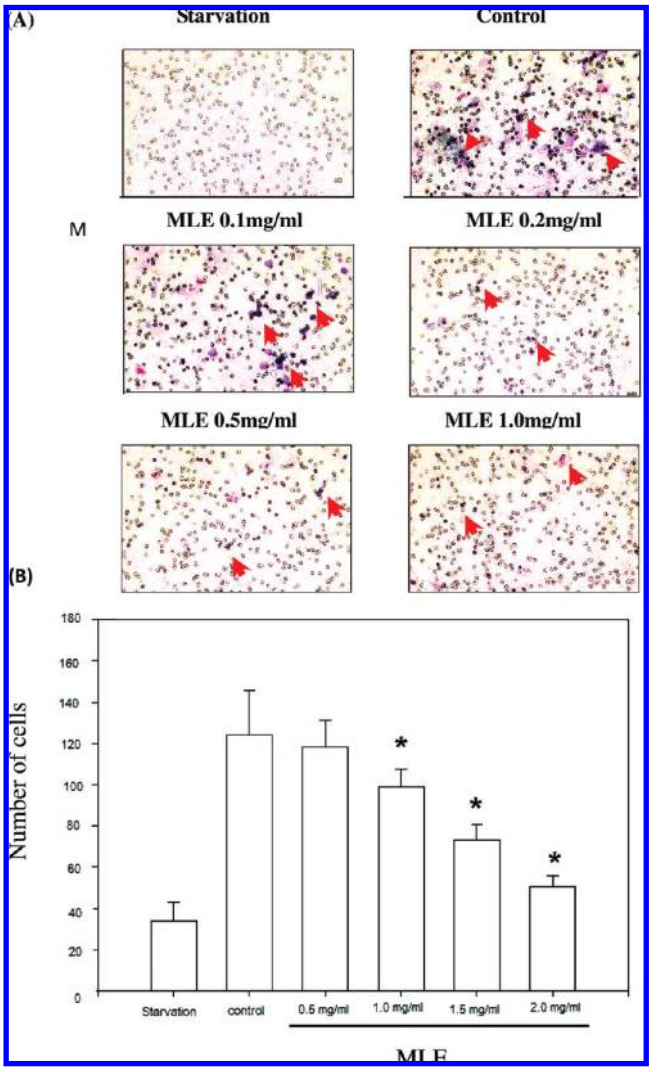

Figure 4. Effect of MLE on the migration of A7r5 cells by the Boyden chamber assay. (**A**) Cells that had invaded to the lower surface of the membranes were fixed with methanol and stained with Giemsa. (**B**) Quantitative assessment of the mean number of cells. MLE inhibited cell migration in a dose-dependent manner. Data are reported as the means ± SD of 3 independent experiments. (*$p < 0.001$, as compared with that of the control group).

were performed. To avoid cytotoxicity effects, we treated A7r5 cells with 0.05, 0.1, 0.2, 0.5, or 1.0 mg/mL of MLE for 72 h. In the wound healing assay, vehicle-treated control cells migrated into the denuded areas. In contrast, cells in the wound area decreased markedly in the presence of 1 mg/mL of MLE (**Figure 3**). As shown by the Boyden chamber assay, a decrease in cells on the lower chamber membrane was observed for MLE-treated cells compared with that in vehicle-control cells (**Figure 4**). Quantitative analysis indicated that MLE decreased the cell motility in a dose-dependent manner. Our results indicated that a low MLE dose could inhibit the motility of smooth muscle cells.

Noncytotoxic Doses of MLE Inhibited VSMC MMP-2 Secretion and Diminished the FAK/PI 3-kinase/Small G Protein Pathway. Zymography analysis was used to investigate whether MLE altered the secretions of MMP-2 and MMP-9. **Figure 5** showed that, in the presence of 0.05, 0.1, 0.2, 0.5, or 1.0 mg/mL of MLE, MMP-2 and MMP-9 activities were inhibited by MLE in a dose- and time dependent manner on the basis of the results of the gelatin zymography assay. It is well known that focal adhesion kinase (FAK)/PI 3-kinase signaling is involved in the regulation

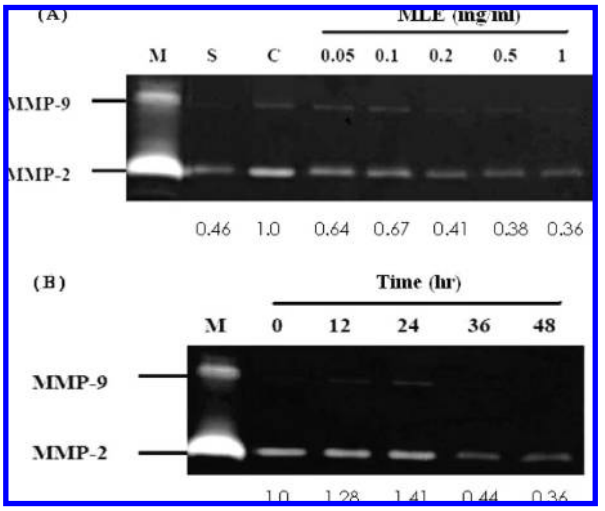

Figure 5. Effect of MLE on MMP-9 and MMP-2 activity of A7r5 cells by the gelatin zymography assay. (**A**) The activity of MMP-2 and MMP-9 was inhibited by MLE in a dose-dependent manner. (**B**) The activity of MMP-2 and MMP-9 was inhibited by MLE in a time-dependent manner. M, marker; S, starvation; C, control.

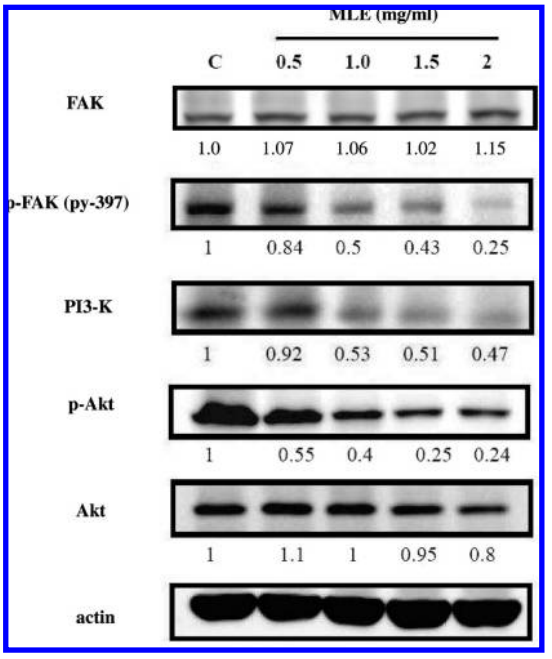

Figure 6. Effect of MLE on protein expression and phosphorylation of FAK and Akt. MLE inhibited the protein expression and phosphorylation of FAK and Akt in a dose-dependent manner. Actin was used as a loading control. C: control.

of cell migration. To highlight the mechanisms of antimigration effects of MLE on smooth muscle cells, the expressions and/or activities of these proteins were measured by Western blot analysis. In the presence of MLE, phosphorylated FAK (phosphorylation at Tyr-397) was decreased in a dose-dependent manner, whereas the protein level of FAK remained unchanged. MLE decreased the protein levels of Ras and PI 3-kinase (**Figure 6**), which subsequently inhibits the activity of its downstream target, FAK. The Rho small G protein family, including Rho A, Rac-1, and Cdc42, plays an important role in actin cytoskeleton remodeling and cell migration. To assess whether Rho family proteins were involved in the decreased cell migration

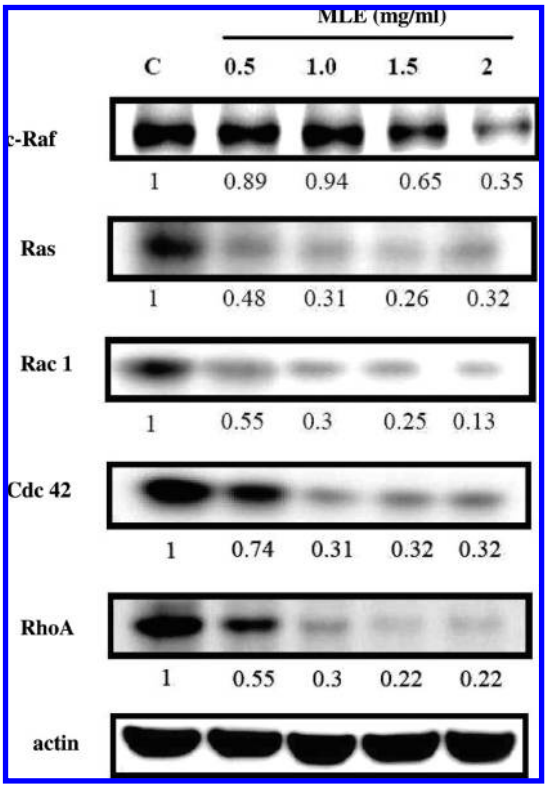

Figure 7. Effect of MLE on the expression of small G proteins. MLE inhibited the protein expression of c-Raf, Ras, Rac1, Cdc42, and RhoA in a dose-dependent manner. Actin was used as a loading control.

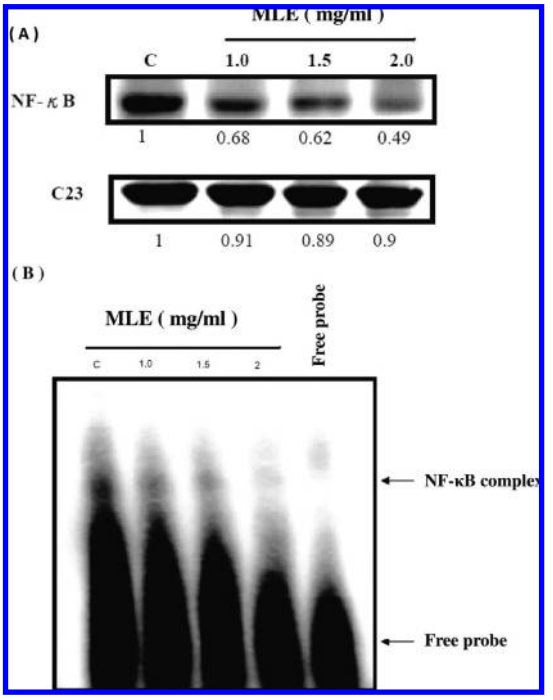

Figure 8. Effects of MLE on NF-κB DNA binding. (**A**)The protein level of NF-κB was inhibited by MLE. C23 is the nuclear control. (**B**) NF-κB DNA binding activity was inhibited by MLE.

by MLE, the levels of Rho family proteins Rho A, Rac-1, and Cdc42 were determined using specific antibodies. The protein levels of Rho A, Rac-1, and Cdc42 were decreased in proportion to increased concentrations of MLE (**Figure 7**). Last, **Figure 8**

shows that MLE inhibited the protein level of NF-κB DNA binding activity on the basis of the electrophoretic mobility shift assay (EMSA).

Atherosclerosis is a multistep, chronic inflammatory process that involves interactions between various soluble mediators, monocytes, endothelial cells, and smooth muscle cells. Endothelial dysfunction is the initial step that can be caused by various stimuli, such as hyperglycemia, dyslipidemia, smoking, hypertension, and generation of free radicals. Subsequently, adhesion molecules and chemotactic cytokines will attract monocytes and T cells that transmigrate into the intima of the vascular wall. Thereafter, monocytes take up oxidized LDL and make a transition to foam cells, which is the early atherosclerotic lesion.

Monocyte-derived cytokines and growth factors will further affect the vascular wall by stimulating SMC proliferation and migration. Monocytes may also secrete matrix metalloproteinases that lead to plaque instability and rupture (*20*). The migration of VSMCs from the media into the intima is a key event in the development and progression of many vascular diseases (*21*). From in vivo experiments, cell migration is a highly predictable consequence of mechanical injury to the blood vessel. Restenosis after PCI is caused primarily by the dysfunction of VSMCs, including migration into and proliferation in the intima (*22*).

Recent reports have also indicated that polyphenols (catechin, quercetin, EGCG, and resveratrol) can inhibit vascular smooth muscle cell proliferation and migration (*23*−*26*). According to these reports, we inferred that these polyphenols may be the main components of MLE and might inhibit the migration of vascular smooth muscle cells.

The migration of smooth muscle cells from medial to intimal spaces contributes to the formation of atherosclerosis (*27*). Focal adhesion kinase (FAK) can be activated in response to diverse stimuli and plays an important role in the proliferation and migration of cells (*28*). Activated FAK induced PI 3-kinase is required for the production of matrix metalloproteinases (MMPs) (*29*). MMPs, a family of proteinases, promote the degradation of extracellular cellular matrix, which, in turn, facilitates cell migration (*30*). Owing to their roles in migration, FAK and MMPs were shown to be overexpressed in tumors with highly metastatic ability (*31*, *32*). Shibata et al. have shown that stimulated ovarian cancer cells with fibronectin increased the secretion of MMP-9, while dominant negative Ras and antisense oligonucleotide for FAK abolished this phenomenon (*33*). Similar results also indicated that FAK/PI 3-kinase signaling may be involved in fibronectin-induced MMP-2 and MMP-9 activities. Rho, a small G protein family protein, including Rho, Rac1, and Cdc42, which regulates cytoskeleton remodeling, was also involved in smooth muscle cell migration. It has been shown that Rho and its downstream target Rho kinase mediated thrombin-induced vascular smooth muscle cell migration.

Endothelial dysfunction elicited by oxidized LDL and hyperglycemia have contributed to atherosclerosis. Mulberry leaf aqueous fractions were reported to inhibit TNF (tumor necrosis factor)-α-induced nuclear factor κB (NF-κB) activation and lectin-like oxidized LDL receptor-1 (LOX-1) expression in vascular endothelial cells (*34*). Besides, mulberry leaf treatment was also shown to be beneficial for metabolic syndrome by increasing the expression of adiponectin, and decreasing the expression of TNF-α, MCP-1, macrophage markers, and NADPH oxidase subunit in white adipose tissue in db/db mice (*35*). Our results indicated that MLE treatment not only decreased the activity of the FAK/PI 3-kinase pathway but also reduced the expressions of Rho, Rac1, and Cdc42. Our results suggested that the FAK/PI 3-kinase pathway and Rho family proteins were involved in MLE-induced suppression of migration. The activity of NF-κB was also inhibited by MLE. Our study showed that the major component of MLE was polyphenol (44.82%, quercetin as the standard of the polyphenol content assay). Polyphenols were reported to have many biochemical activities, and it has never been reported before that polysaccharide, protein, or lipid had any impact on the migration of VSMCs. Thus, the inhibitory effect of MLE on the migration of VSMCs was attributed to the polyphenol component of MLE.

In summary, these in vitro studies demonstrated molecular mechanisms by which MLE effectively inhibits the migration of VSMCs. This inhibitory effect of MLE is achieved by acting on multiple signals upstream of MMP-2 and MMP-9, including the block of small GTPase and Akt/NF-κB signals. Besides, MLE can interfere with the rearrangement of the actin cytoskeleton by decreasing the expression of p-FAK, thus inhibiting the migration of VSMC. These mechanisms could explain some of the antiatherosclerotic effects of MLE.

LITERATURE CITED

(1) Thom, T.; Haase, N.; Rosamond, W.; Howard, V. J.; Rumsfeld, J.; Manolio, T.; Zheng, Z. J.; Flegal, K.; O'Donnell, C.; Kittner, S.; Lloyd-Jones, D.; Goff, D. C.Jr.; Hong, Y.; Adams, R.; Friday, G.; Furie, K.; Gorelick, P.; Kissela, B.; Marler, J.; Meigs, J.; Roger, V.; Sidney, S.; Sorlie, P.; Steinberger, J.; Wasserthiel-Smoller, S.; Wilson, M.; Wolf, P. American Heart Association Statistics Committee and Stroke Statistics Subcommittee. Heart disease and stroke statistics--2006 update: a report from the American Heart Association Statistics Committee and Stroke Statistics Subcommittee. *Circulation* **2006**, *113*, e85–e151.

(2) Visioli, F.; Borsani, L.; Galli, C. Diet and prevention of coronary heart disease: the potential role of phytochemicals. *Cardiovasc. Res.* **2000**, *47*, 419–425.

(3) Liu, L. K.; Lee, H. J.; Shih, Y. W.; Chyau, C. C.; Wang, C. J. Mulberry anthocyanin extracts inhibit LDL oxidation and macrophage-derived foam cell formation induced by oxidative LDL. *J. Food Sci.* **2008**, *73*, H113–H121.

(4) Asano, N.; Yamashita, T.; Yasuda, K.; Ikeda, K.; Kizu, H.; Kameda, Y.; Kato, A.; Nash, R. J.; Lee, H. S.; Ryu, K. S. Polyhydroxylated alkaloids isolated from mulberry trees (*Morus alba* L.) and silkworms (*Bombyx mori* L.). *J. Agric. Food Chem.* **2001**, *49*, 4208–4213.

(5) Kimura, T.; Nakagawa, K.; Kubota, H.; Kojima, Y.; Goto, Y.; Yamagishi, K.; Oita, S.; Oikawa, S.; Miyazawa, T. Food-grade mulberry powder enriched with 1-deoxynojirimycin suppresses the elevation of postprandial blood glucose in humans. *J. Agric. Food Chem.* **2007**, *55*, 5869–5874.

(6) El-Beshbishy, H. A.; Singab, A. N.; Sinkkonen, J.; Pihlaja, K. Hypolipidemic and antioxidant effects of *Morus alba* L. (Egyptian mulberry) root bark fractions supplementation in cholesterol-fed rats. *Life Sci.* **2006**, *78*, 2724–2733.

(7) Isabelle, M.; Lee, B. L.; Ong, C. N.; Liu, X.; Huang, D. Peroxyl radical scavenging capacity, polyphenolics, and lipophilic antioxidant profiles of mulberry fruits cultivated in southern China. *J. Agric. Food Chem.* **2008**, *56*, 9410–9416.

(8) Doi, K.; Kojima, T.; Fujimoto, Y. Mulberry leaf extract inhibits the oxidative modification of rabbit and human low density lipoprotein. *Biol. Pharm. Bull.* **2000**, *23*, 1066–1071.

(9) Harauma, A.; Murayama, T.; Ikeyama, K; Sano, H.; Arai, H.; Takano, R.; Hara, S.; Kamei, K.; Yokode, M. Mulberry leaf power prevents atherosclerosis in apolipoprotein E-deficient mice. *Biochem. Biophys. Res. Commun.* **2007**, *358*, 751–756.

(10) Andallu, B.; Suryakantham, V.; Lakshmi Srikanthi, B.; Reddy, G. K. Effect of mulberry (*Morus indica* L.) therapy on plasma and erythrocyte membrane lipid in patients with type 2 diabetes. *Clin. Chim. Acta* **2001**, *314*, 47–53.

(11) Andallu, B.; Varadacharyulu, N. Antioxidant role of mulberry (*Morus indica* L. Cv. Anantha) leaves in streptozotocin-diabetic rats. *Clin. Chim. Acta* **2003**, *338*, 3–10.

(12) Cary, L. A.; Han, D. C.; Guan, J. L. Integrin-mediated signal transduction pathways. *Histol. Histopathol.* **1999**, *14*, 1001–1009.
(13) Cary, L. A.; Chang, J. F.; Guan, J. L. Stimulation of cell migration by overexpression of focal adhesion kinase and its association with Src and Fyn. *J. Cell Sci.* **1996**, *109*, 1787–1794.
(14) Seasholtz, T. M.; Majumdar, M.; Kaplan, D. D.; Brown, J. H. Rho and Rho kinase mediate thrombin-stimulated vascular smooth muscle cell DNA synthesis and migration. *Circ. Res.* **1999**, *84*, 1186–1193.
(15) De Martin, R.; Hoeth, M.; Hofer-Warbinek, R.; Schmid, J. A. The transcription factor NF-kappa B and the regulation of vascular cell function. *Arterioscler., Thromb., Vasc. Biol.* **2000**, *20*, e83–88.
(16) Bond, M.; Fabunmi, R. P.; Baker, A. H.; Newby, A. C. Synergistic upregulation of metalloproteinase-9 by growth factors and inflammatory cytokines: an absolute requirement for transcription factor NF-kappa B. *FEBS Lett.* **1998**, *435*, 29–34.
(17) van Leeuwen, R. T. J. Extracellular proteolysis and the migrating vascular smooth muscle cell. *Fibrionolysis* **1996**, *10*, 59–74.
(18) Goncharova, E. A.; Ammit, A. J.; Irani, C.; Carroll, R. G.; Eszterhas, A. J.; Panettieri, R. A.; Krymskaya, V. P. PI3K is required for proliferation and migration of human pulmonary vascular smooth muscle cells. *Am. J. Physiol. Lung Cell Mol. Physiol.* **2002**, *283*, L354–363.
(19) Khwaja, A. Akt is more than just a Bad kinase. *Nature* **1999**, *401*, 33–34.
(20) Lee, R. T.; Libby, P. The unstable atheroma. *Arterioscler., Thromb., Vasc. Biol.* **1997**, *17*, 1859–1867.
(21) Casscells, W. Migration of smooth muscle and endothelial cells. Critical events in restenosis. *Circulation* **1992**, *86*, 723–729.
(22) Clowes, A. W.; Schwartz, S. M. Significance of quiescent smooth muscle migration in the injured rat carotid artery. *Circ. Res.* **1985**, *56*, 139–145.
(23) Ekshyyan, V. P.; Hebert, V. Y.; Khandelwal, A.; Dugas, T. R. Resveratrol inhibits rat aortic vascular smooth muscle cell proliferation via estrogen receptor dependent nitric oxide production. *J. Cardiovasc. Pharmacol.* **2007**, *50*, 83–93.
(24) Lo, H. M.; Hung, C. F.; Huang, Y. Y.; Wu, W. B. Tea polyphenols inhibit rat vascular smooth muscle cell adhesion and migration on collagen and laminin via interference with cell-ECM interaction. *J. Biomed. Sci.* **2007**, *14*, 637–645.
(25) Perez-Vizcaino, F.; Bishop-Bailley, D.; Lodi, F.; Duarte, J.; Cogolludo, A.; Moreno, L.; Bosca, L.; Mitchell, J. A.; Warner, T. D. The flavonoid quercetin induces apoptosis and inhibits JNK activation in intimal vascular smooth muscle cells. *Biochem. Biophys. Res. Commun.* **2006**, *346*, 919–925.
(26) Won, S. M.; Park, Y. H.; Kim, H. J.; Park, K. M.; Lee, W. J. Catechins inhibit angiotensin II-induced vascular smooth muscle cell proliferation via mitogen-activated protein kinase pathway. *Exp. Mol. Med.* **2006**, *38*, 525–534.
(27) Glass, C. K.; Witztum, J. L. Atherosclerosis. the road ahead. *Cell* **2001**, *104*, 503–516.
(28) Parsons, J. T. Focal adhesion kinase: the first ten years. *J. Cell Sci.* **2003**, *116*, 1409–1416.
(29) Zeng, Z. Z.; Jia, Y.; Hahn, N. J.; Markwart, S. M.; Rockwood, K. F.; Livant, D. L. Role of focal adhesion kinase and phosphatidylinositol 3′-kinase in integrin fibronectin receptor-mediated, matrix metalloproteinase-1-dependent invasion by metastatic prostate cancer cells. *Cancer Res.* **2006**, *66*, 8091–8099.
(30) McCawley, L. J.; Matrisian, L. M. Matrix metalloproteinases: multifunctional contributors to tumor progression. *Mol. Med. Today* **2000**, *6*, 149–156.
(31) Cockett, M. I.; Murphy, G.; Birch, M. L.; O'Connell, J. P.; Crabbe, T.; Millican, A. T.; Hart, I. R.; Docherty, A. J. Matrix metalloproteinases and metastatic cancer. *Biochem. Soc. Symp.* **1998**, *63*, 295–313.
(32) Kornberg, L. J. Focal adhesion kinase and its potential involvement in tumor invasion and metastasis. *Head Neck* **1998**, *20*, 745–752.
(33) Shibata, K.; Kikkawa, F.; Nawa, A.; Thant, A. A.; Naruse, K.; Mizutani, S.; Hamaguchi, M. Both focal adhesion kinase and c-Ras are required for the enhanced matrix metalloproteinase 9 secretion by fibronectin in ovarian cancer cells. *Cancer Res.* **1998**, *58*, 900–903.
(34) Shibata, Y.; Kume, N.; Arai, H.; Hayashida, K.; Inui-Hayashida, A.; Minami, M.; Mukai, E.; Toyohara, M.; Harauma, A.; Murayama, T.; Kita, T.; Hara, S.; Kamei, K.; Yokode, M. Mulberry leaf aqueous fractions inhibit TNF-alpha-induced nuclear factor kappaB (NF-kappaB) activation and lectin-like oxidized LDL receptor-1 (LOX-1) expression in vascular endothelial cells. *Atherosclerosis* **2007**, *193*, 20–27.
(35) Sugimoto, M.; Arai, H.; Tamura, Y.; Murayama, T.; Khaengkhan, P.; Nishio, T.; Ono, K.; Ariyasu, H.; Akamizu, T.; Ueda, Y.; Kita, T.; Harada, S.; Kamei, K.; Yokode, M. Mulberry leaf ameliorates the expression profile of adipocytokines by inhibiting oxidative stress in white adipose tissue in db/db mice. *Atherosclerosis* **2009**, *204*, 388–394.

Received July 31, 2009. Revised manuscript received August 31, 2009. Accepted September 02, 2009. This work was supported by a research fund from Chung Shan Medical University Hospital, Taichung, Taiwan, (CSH-2009-C-005) and National Science Council, Taiwan, (NSC 96-2628-B-040-022-MY3).